Journal of Biomechanics 193 (2025) 112993

Contents lists available at ScienceDirect

Journal of Biomechanics

journal homepage: www.elsevier.com/locate/jbiomech

Short communication

Stochastic modelling of muscle control during shoulder abduction

Alex Bersani [a,*], Saulo Martelli [b,c], Maxence Lavaill [b,c], Giorgio Davico [a]

[a] Department of Industrial Engineering, Alma Mater Studiorum – University of Bologna, Bologna, Italy
[b] School of Mechanical, Medical and Process Engineering, Queensland University of Technology, Brisbane, Australia
[c] Centre for Biomedical Technologies, Queensland University of Technology, Brisbane, Australia

ARTICLE INFO

Keywords:
Shoulder modelling
Suboptimal control
Stochastic muscle recruitment
Stochastic approach
Electromyography

ABSTRACT

The intrinsic variability of the shoulder joint motion is a critical factor in the characterisation of the shoulder joint. However, traditional computational approaches struggle to account for it. On the other hand, the stochastic approach allows to identify a set of plausible solutions. In this study, the Myobolica toolbox, which yielded promising results in the lower limb, was employed to simulate a shoulder abduction, with twofold aims: to assess its generalisability to other joints, and to evaluate an electromyography (EMG)-informed version of Myobolica.

Publicly available kinematics, EMG, and glenohumeral (GH) joint force data measured by an instrumented implant on a 64-year-old man executing three weighted shoulder abductions were used. A previously developed shoulder musculoskeletal model was employed to compute stochastic simulations informed and not with EMG data, sampling 1×10^5 solutions every 30 timeframes. The predicted GH joint force were compared to the experimental data, and the variance in the solutions across simulations was computed.

Overall, the correlation between the GH joint force predicted by Myobolica and the experimental values increased when the EMG-based constraint was applied (from approximately $R^2 = 0.06$, RMSE = 1.82 BW to $R^2 = 0.6$, RMSE = 0.73 BW when all available EMG data were employed). Using EMG led to a reduction (from 2.3 to 0.65 BW) in the solution bandwidths.

Providing EMG data to inform the simulations helped improve their accuracy. However, the results obtained otherwise remain promising. Additional work is required to minimize the computational cost of the Myobolica approach. A consistency gap between experimental data and the model is reported.

1. Introduction

The glenohumeral joint is central in the execution of activities of daily living (Bergmann et al., 2007; Klemt et al., 2018). This is particularly evident in individuals with non-healthy shoulders, whose motion may be severely compromised (Bruttel et al., 2019; Magermans et al., 2005). In this scenario, the importance of having a reasonable estimation of musculoskeletal biomarkers, such as muscle or joint contact forces, for treatment and rehabilitation purposes (Jonkers et al., 2023; Killen et al., 2020) or to optimise prosthetic design (Veeger et al., 2006), becomes apparent.

Traditional methods to predict musculoskeletal forces include static optimisation and electromyography (EMG)-informed approaches. The first one assumes that muscles are controlled according to a physiological criterion modelled through a cost function to be optimised (Crowninshield and Brand, 1981; Nikooyan et al., 2010) but tend to underestimate joint forces (Kian et al., 2019; Nikooyan et al., 2010) by discouraging muscle co-contraction (Croci et al., 2023; Wickham et al., 2010), and the second one is often adopted to ensure the solution tracks experimental muscle excitations (Davico et al., 2022; Veerkamp et al., 2019) but may suffer from the intrinsic problems of the EMG acquisition (Besomi et al., 2020). In addition, optimal control methods where different optimisation algorithms are used to solve complex tasks and to perform both inverse and forward (Febrer-Nafría et al., 2023) dynamics simulations, but can show convergence and high CPU time issues (Febrer-Nafría et al., 2023; Puchaud et al., 2023).

Alternatively, in the last decade, a stochastic modelling approach has been proposed to solve the muscle recruitment problem while accounting for muscle co-contractions, modelling errors and the muscle control intrinsic variability (Johnson et al., 2022; Martelli et al., 2013). Based on the uncontrolled manifold theory (Scholz and Schöner, 1999), the stochastic approach relies on Bayesian statistics and a Monte Carlo

* Corresponding author.
E-mail addresses: alex.bersani2@unibo.it (A. Bersani), saulo.martelli@qut.edu.au (S. Martelli), maxence.lavaill@qut.edu.au (M. Lavaill), giorgio.davico@unibo.it (G. Davico).

https://doi.org/10.1016/j.jbiomech.2025.112993
Accepted 30 September 2025
Available online 1 October 2025
0021-9290/© 2025 The Author(s). Published by Elsevier Ltd. This is an open access article under the CC BY license (http://creativecommons.org/licenses/by/4.0/).

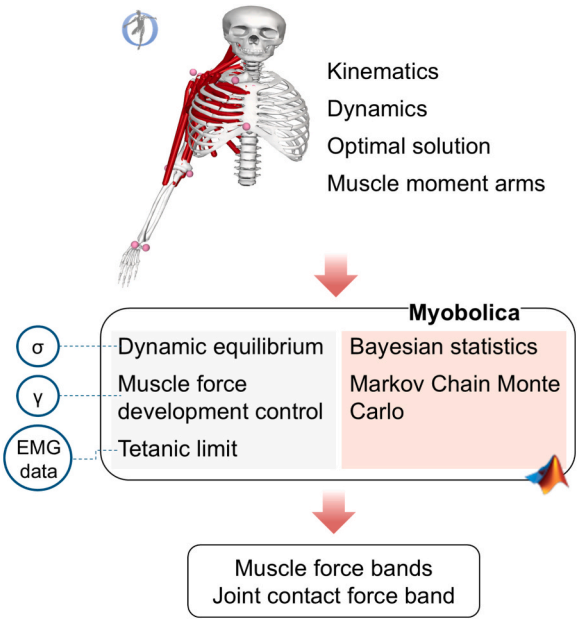

Fig. 1. Summary of the workflow. Biomechanical parameters are extracted from the musculoskeletal model; then, the stochastic approach (Myobolica) is adopted to predict bands of plausible muscle and joint contact forces.

Table 1
Overview of all simulations performed and corresponding simulation labels. Columns show whether the muscle-specific (MS) gamma parameter and each available muscle EMG data are exploited.

Simulation	Muscle-specific gamma parameter	Deltoid EMG	Biceps EMG	Triceps EMG	Trapezius EMG
Default					
MS gamma parameter	✓				
Delt. EMG	✓	✓			
Bic. EMG	✓		✓		
Tric. EMG	✓			✓	
Trap. EMG	✓				✓
All EMGS	✓	✓	✓	✓	✓

(or Markov Chain Monte Carlo) algorithm to sample a band of feasible solutions (Amankwah et al., 2024; Heino et al., 2010; Johnson et al., 2022), albeit requiring a non-negligible computation time. Adopted various times to estimate the impact of a sub-optimal control (Martelli et al., 2015; van Veen et al., 2020; Viceconti et al., 2021), the stochastic approach has been recently improved by constraining time changes of muscle forces either explicitly (Amankwah et al., 2024; Bersani et al., 2024) or by modulating the peak muscle force boundaries (Bennett et al., 2022). Constraining the force generation rate led to promising results in the lower limb (Bersani et al., 2024), but those are yet to be generalised for application to other joints. In addition, the possibility to combine EMG-informed and stochastic modelling approaches towards more physiologically plausible estimates remains a largely unexplored scientific space. The aim of the present study was twofold: i) to evaluate the Myobolica toolbox to model muscle control of the shoulder joint; ii) to understand the impact of adding EMG signals as a new physiological constraint to the proposed stochastic approach.

2. Materials and methods

2.1. Experimental data

The experimental data employed in this study were collected on a 64-year-old man (labelled S2R) implanted with an instrumented right shoulder prosthesis, part of a publicly available dataset (Nikooyan et al., 2010; Veeger and van der Helm, 2023). The dataset included motion capture data, the EMG signals from seven superficial muscles, and the in vivo glenohumeral joint contact force measured by the instrumented implant (Nikooyan et al., 2012). A single trial, composed of three consecutive shoulder slow abductions while the subject held a 2.4 kg weight, was selected for the simulations.

The EMG data were filtered to compute the linear envelopes of the signals by implementing a zero-lag 8th order Butterworth filter (40–400 Hz), followed by a full-wave rectification and a zero-lag 8th order low-pass Butterworth filter at 5 Hz, and normalised to the maximum value from the available functional, force and maximal voluntary contraction tests (Lavaill et al., 2024).

The musculoskeletal model was inherited from previous work (Lavaill et al., 2023). It consists of seven bodies (thorax, clavicle, scapula, humerus, ulna, radius, and hand), eleven degrees of freedom (three for the sternoclavicular, the acromioclavicular and the glenohumeral joints, one for the elbow, and the radioulnar) and 91 muscle–tendon actuators ("Millard2012EquilibriumMuscle" muscle model (Millard et al., 2013)).

2.2. Simulations workflow

An outline of the workflow is summarised in Fig. 1. The open-source software OpenSim 4.1 (Delp et al., 2007) was employed to estimate model kinematics, kinetics, and the muscle lever arms. The OpenSim static optimisation and joint reaction tools were used to predict an optimal solution for the muscle and joint contact forces, which was later used as an initial tentative solution to Myobolica for the stochastic simulations. Due to the limited actuation of the thoracoscapular joint made by the adopted model (the Delf Shoulder and Elbow Model, DSEM) (Lavaill et al., 2023), reserve actuators stronger than those recommended in OpenSim guidelines (Hicks et al., 2015) were required for the sternoclavicular, the acromioclavicular, the elbow, and the radioulnar degrees of freedom.

Stochastic simulations were performed within Myobolica (Amankwah et al., 2024; Bersani et al., 2024) through MATLAB

Table 2
R^2 and RMSE between Myobolica median solutions and the experimental data for the three trials, and the GH joint contact force average solution space among the three trials.

Simulation	R^2			RMSE [BW]			Solution space average Bandwidth [BW]		
	Trial 1	Trial 2	Trial 3	Trial 1	Trial 2	Trial 3	Trial 1	Trial 2	Trial 3
Default	0.23	−0.03	−0.03	1.70	1.81	1.94	2.24 ± 0.67	2.31 ± 0.76	2.35 ± 0.80
MS gamma parameter	0.26	−0.08	0.09	1.10	1.46	1.10	1.25 ± 0.40	1.49 ± 0.6	1.33 ± 0.47
Delt. EMG	0.45	0.29	0.61	1.10	1.10	0.907	1.40 ± 0.49	1.32 ± 0.47	1 ± 0.46
Bic. EMG	0.39	0.006	0.19	1.04	1.35	1.11	1.26 ± 0.39	1.50 ± 0.48	1.31 ± 0.42
Tric. EMG	0.32	0.09	0.18	1.38	1.46	1.49	1.47 ± 0.48	1.48 ± 0.53	1.48 ± 0.57
Trap. EMG	0.16	−0.06	−0.09	0.88	1.07	0.97	1.20 ± 0.45	1.34 ± 0.52	1.17 ± 0.52
All EMGs	0.61	0.42	0.76	0.77	0.78	0.63	0.72 ± 0.24	0.67 ± 0.26	0.55 ± 0.25

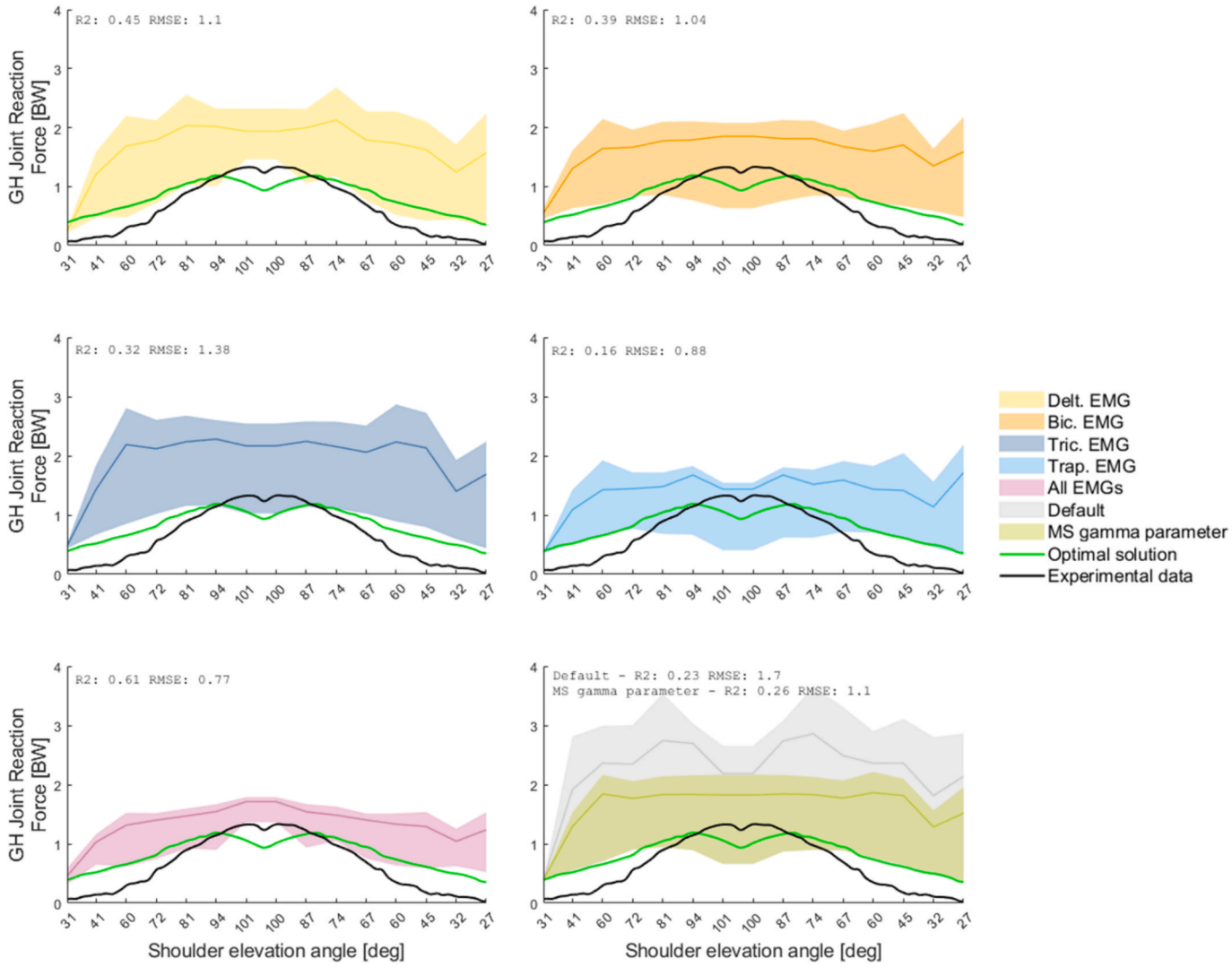

Fig. 2. Comparison of the first trial GH joint contact forces predicted by Myobolica (shaded areas), optimal solution (green), and experimentally measured data (black). R^2 and RMSE between the first trial Myobolica median solutions and the experimental data are reported. Myobolica solutions were computed, in order, enforcing only deltoid muscles EMG (yellow), only biceps EMG (orange), only triceps EMG (dark blue), only trapezius EMG (light blue), all the previously mentioned EMGs (light purple), and without enforcing any muscle EMG (earls green); all the previously mentioned simulation were obtained normalising the gamma parameter. The default Myobolica result, without enforcing any muscle EMG or normalising gamma, is reported in grey. (For interpretation of the references to colour in this figure legend, the reader is referred to the web version of this article.)

(v2021b). Myobolica works by sampling the posterior probability distribution function of the unknown variable (i.e., muscle forces) estimated with Bayesian statistics (Eq. (1) (Amankwah et al., 2024).

$$\pi(F_{mus}|M)\alpha\pi pr(F_{mus})\pi(M|F_{mus}) \quad (1)$$

where

$$M = B \times F_{mus} + \varepsilon \quad (2)$$

$$\varepsilon = N(0, \sigma^2) \quad (3)$$

$$F_{mus,t} - F_{mus,t-1} = \eta t \quad (4)$$

$$\eta t = N(0, \gamma^2) \quad (5)$$

With F_{mus} as the muscle forces vector, M the joint torques vector, B the matrix of muscle lever arms, and "N" representing a Gaussian distribution with 0 mean and σ or γ as the standard deviations. In the present work, the parameter sigma (σ), modelling noise and uncertainties in the equilibrium condition equation (Eqs. (2) and (3)), was set to 0.12 as per (Bersani et al., 2024), while the gamma (γ), which models how fast each muscle is able to generate force (Eqs. (4) and (5)), was set to 0.45, based on the rate of force development (RFD) derived from the literature experimental data (Davico et al., 2024) and normalised to the current simulation timeframe, as per (Bersani et al., 2024).

Overall, after internal tests to reduce the computational cost while minimising the loss of accuracy, 1×10^5 solutions were sampled, and the system equations were evaluated every 30 timeframes. Each solution consisted of a set of 91 muscle forces.

We then updated the gamma values for the muscles that were modelled with multiple actuators (e.g., the deltoids muscle is modelled with 15 actuators), by normalising the experimentally determined gamma value to the number of actuators (Supplementary Table S1) to address the possible overestimated force generation issue when assigning a gamma value, representative of a whole muscle behaviour, to each subcomponent of the modelled muscle, and run Myobolica a second time. Following, we performed a new batch of stochastic simulations, informed by EMG data. In this case, the initial tentative solution was replaced by the EMG-derived force for the deltoids, triceps, biceps, and trapezius muscles. The latter was obtained by multiplying the processed

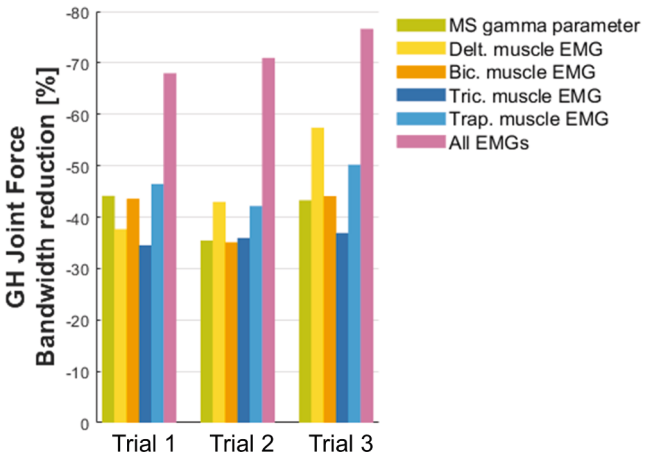

Fig. 3. The reduction of the GH joint contact force solution space from the Default simulation to each subsequent simulation for the three trials. Myobolica solutions were computed, in order, without enforcing any muscle EMG (earls green), enforcing only deltoid muscles EMG (yellow), only biceps EMG (orange), only triceps EMG (dark blue), only trapezius EMG (light blue), and all the previously mentioned EMGs (light purple); all the previously mentioned simulation were obtained normalising the gamma parameter. (For interpretation of the references to colour in this figure legend, the reader is referred to the web version of this article.)

and normalised EMG signal by the maximal isometric force of the specific muscle. The operating boundaries for the sampler were modulated assuming a 50 % error for the EMG-derived force. The error value has been selected to provide the sampler with smaller boundaries than the default Myobolica simulation without over-constraining the system.

For all simulations (Table 1), the resulting glenohumeral joint contact force solution space was estimated using the OpenSim API for MATLAB.

2.3. Data analysis

The resulting glenohumeral (GH) joint contact force solutions were sorted in ascending order, normalised to the subject's body weight, with the median solutions and range between the minimum and maximum solutions plotted against the shoulder elevation angle for consistency with the literature (Lavaill et al., 2024). The median solution was plotted as well. Solution profiles are reported only for the first trial for conciseness; the remaining are reported in the Supplementary file.

To assess how the stochastic approach performed, we compared the output of the various simulations to the experimental GH joint contact force by computing the R^2 index and the root mean square error (RMSE), as well as the overall solution space area (calculated as the top solution minus the bottom solution for each timeframe). In the Results section, average values across the three trials are reported, with each trial's values reported in Table 2. To assess the impact of the EMG constraint on the solutions, we compared the average bandwidth of the EMG-informed and Default stochastic simulations (reported in the Supplementary Files only).

3. Results

The use of EMG data to inform the stochastic simulations was associated with a general improvement in the output from Myobolica (Fig. 2). The resulting solutions better approximated the implant data ($R^2 > 0.16$, RMSE < 1.38 BW), compared to the simulations where no EMG data were employed. The best results were achieved when data from all four muscle groups were utilised (All EMGs simulation, $R^2 = 0.6$ and RMSE $= 0.73$ BW, on average across the three trials) (Table 2).

Not enforcing EMG constraints led to the lowest correlation with the experimentally measured joint force in the Default simulation, as reported in Fig. 2. Updating the gamma parameter (MS gamma parameter simulation) led to a substantial reduction in the RMSE ($\sim$ 30 % from the Default simulation), but left almost unaltered and close to 0 the R^2 value (0.06 vs 0.09, Table 2). Informing the activity of a single muscle with EMG data led to improvements less conspicuous than in the simulation where all EMG data are utilised ($R^2 \leq 0.45$ and RMSE ≤ 1.03 BW, where the best metrics were observed in Delt. EMG simulation)(Fig. 2).

The width of the predicted GH joint force solution space always decreased when adding the new EMG-based constraint (Fig. 3), reaching a reduction of $\sim$ 70 % (from the Default simulation) in the All EMGs simulation (Table 2). Less marked reductions (up to 40 %) were observed when single muscles were informed by EMG data (Fig. 3).

4. Discussion

In this work, a novel stochastic approach was employed to simulate a shoulder abduction task, aiming to test the feasibility of applying Myobolica to predict a spectrum of plausible solutions for the shoulder joint and seeking to evaluate the impact of a new physiological constraint based on EMG data. To this end, publicly available data and a previously developed musculoskeletal model were used. In a model such as the shoulder, characterised by high muscle redundancy required to permit a variety of movements, including more information in the model by adding EMG data as a constraint may reduce the variance of the spectrum (Figs. 2 and 3). The improvement changes with the input, likely depending on model sensitivity and measurement errors. The deltoid muscle played a major role in the task, significantly influencing the shape of the predicted solution space. Also, constraining muscles less active in the optimal solution (e.g., biceps and triceps) resulted in a marked impact. In addition, results showed how modelling each actuator's velocity of force generation can become relevant to significantly reduce the solution space (Fig. 2 and Table 2). Compared to a previous implementation of the stochastic approach (Metabolica) employed on a shoulder model (Lavaill et al., 2024), we have been able to reach narrower – and potentially more accurate – solution spaces. Myobolica predicted a GH joint contact force solution space from $\sim$ 64 % in the Default up to $\sim$ 90 % in the All EMGs simulation smaller than the solution space predicted by Metabolica in (Lavaill et al., 2024).

A limitation of this work is the computation time of such an approach. More work is needed in the future to improve the computational efficiency of the method and, even though every solution complies with the equilibrium conditions (Eq. (2)) and the physiological constraints (Eq. (4)) and the muscle activation boundaries), to run Myobolica on multiple trials and subjects without recurring to a subsampling. As already pointed out in a previous work (Lavaill et al., 2024), a lack of consistency between the experimental data and the model predictions stands out.

The results showed how small perturbations in muscle control could lead to significantly different joint contact forces, suggesting again the importance of remembering that non-healthy subjects may control muscles in a completely different way than we may hypothesise. Providing a spectrum of solutions – instead of an individual solution – can be more suitable for a clearer glance at the specific subject muscle control.

CRediT authorship contribution statement

Alex Bersani: Writing – original draft, Visualization, Software, Methodology, Formal analysis, Data curation, Conceptualization. **Saulo Martelli:** Writing – review & editing, Software, Resources, Methodology, Conceptualization. **Maxence Lavaill:** Writing – review & editing, Visualization, Methodology. **Giorgio Davico:** Writing – review & editing, Visualization, Software, Resources, Conceptualization.

Declaration of competing interest

The authors declare that they have no known competing financial interests or personal relationships that could have appeared to influence the work reported in this paper.

Acknowledgments

GD received funding from the European Union - NextGenerationEU through the Italian Ministry of University and Research under PNRR - M4C2-I1.3 Project PR_00000019 “HEAL ITALIA” to Marco Viceconti (CUP J33C22002920006). The Australian Research Council (IC190100020, FT180100338) is also gratefully acknowledged. The authors declare that they do not have any financial or personal relationships with other people or organisations that could have inappropriately influenced this study.

Appendix A. Supplementary data

Supplementary data to this article can be found online at https://doi.org/10.1016/j.jbiomech.2025.112993.

References

Amankwah, M., Bersani, A., Calvetti, D., Davico, G., Somersalo, E., Viceconti, M., 2024. Exploring muscle recruitment by Bayesian methods during motion. Chaos, Solitons Fractals 185, 115082. https://doi.org/10.1016/j.chaos.2024.115082.

Bennett, K.J., Pizzolato, C., Martelli, S., Bahl, J.S., Sivakumar, A., Atkins, G.J., Solomon, L.B., Thewlis, D., 2022. a. IEEE Transactions on Biomedical Engineering 69, 2268–2275. Doi: 10.1109/TBME.2022.3141067.

Bergmann, G., Graichen, F., Bender, A., Kääb, M., Rohlmann, A., Westerhoff, P., 2007. In vivo glenohumeral contact forces—Measurements in the first patient 7 months postoperatively. J. Biomech. 40, 2139–2149. https://doi.org/10.1016/j.jbiomech.2006.10.037.

Bersani, A., Amankwah, M., Calvetti, D., Somersalo, E., Viceconti, M., Davico, G., 2024. Myobolica: a stochastic approach to estimate physiological muscle control variability. IEEE Trans. Neural Syst. Rehabil. Eng. pp. https://doi.org/10.1109/TNSRE.2024.3447791.

Besomi, M., Hodges, P.W., Clancy, E.A., Van Dieën, J., Hug, F., Lowery, M., Merletti, R., Søgaard, K., Wrigley, T., Besier, T., Carson, R.G., Disselhorst-Klug, C., Enoka, R.M., Falla, D., Farina, D., Gandevia, S., Holobar, A., Kiernan, M.C., McGill, K., Perreault, E., Rothwell, J.C., Tucker, K., 2020. Consensus for experimental design in electromyography (CEDE) project: Amplitude normalization matrix. J. Electromyogr. Kinesiol. 53, 102438. https://doi.org/10.1016/j.jelekin.2020.102438.

Bruttel, H., Spranz, D.M., Bülhoff, M., Aljohani, N., Wolf, S.I., Maier, M.W., 2019. Comparison of glenohumeral and humerothoracical range of motion in healthy controls, osteoarthritic patients and patients after total shoulder arthroplasty performing different activities of daily living. Gait Posture 71, 20–25. https://doi.org/10.1016/j.gaitpost.2019.04.001.

Croci, E., Warmuth, F., Baum, C., Kovacs, B.K., Nüesch, C., Baumgartner, D., Müller, A. M., Mündermann, A., 2023. Load-induced increase in muscle activity during 30° abduction in patients with rotator cuff tears and control subjects. J. Orthop. Traumatol. 24, 41. https://doi.org/10.1186/s10195-023-00720-8.

Crowninshield, R.D., Brand, R.A., 1981. A physiologically based criterion of muscle force prediction in locomotion. J. Biomech. 14, 793–801. https://doi.org/10.1016/0021-9290(81)90035-X.

Davico, G., Labanca, L., Gennarelli, I., Benedetti, M.G., Viceconti, M., 2024. Towards a comprehensive biomechanical assessment of the elderly combining in vivo data and in silico methods. Front. Bioeng. Biotechnol. 12, 1356417. https://doi.org/10.3389/fbioe.2024.1356417.

Davico, G., Lloyd, D.G., Carty, C.P., Killen, B.A., Devaprakash, D., Pizzolato, C., 2022. Multi-level personalization of neuromusculoskeletal models to estimate physiologically plausible knee joint contact forces in children. Biomech. Model. Mechanobiol. https://doi.org/10.1007/s10237-022-01626-w.

Delp, S.L., Anderson, F.C., Arnold, A.S., Loan, P., Habib, A., John, C.T., Guendelman, E., Thelen, D.G., 2007. OpenSim: open-source software to create and analyze dynamic simulations of movement. IEEE Trans. Biomed. Eng. 54, 1940–1950. https://doi.org/10.1109/TBME.2007.901024.

Febrer-Nafría, M., Nasr, A., Ezati, M., Brown, P., Font-Llagunes, J.M., McPhee, J., 2023. Predictive multibody dynamic simulation of human neuromusculoskeletal systems: a review. Multibody Syst. Dyn. 58, 299–339. https://doi.org/10.1007/s11044-022-09852-x.

Heino, J., Calvetti, D., Somersalo, E., 2010. Metabolica: a statistical research tool for analyzing metabolic networks. Comput. Methods Programs Biomed. 97, 151–167. https://doi.org/10.1016/j.cmpb.2009.07.007.

Hicks, J.L., Uchida, T.K., Seth, A., Rajagopal, A., Delp, S.L., 2015. Is my model good enough? Best practices for verification and validation of musculoskeletal models and simulations of movement. J. Biomech. Eng. 137. https://doi.org/10.1115/1.4029304.

Johnson, R.T., Lakeland, D., Finley, J.M., 2022. Using Bayesian inference to estimate plausible muscle forces in musculoskeletal models. J. Neuroeng. Rehabil. 19, 34. https://doi.org/10.1186/s12984-022-01008-4.

Jonkers, I., Beaucage-Gauvreau, E., Killen, B.A., Gupta, D., Scheys, L., Groote, F.D., 2023. In Silico Biomarkers of Motor Function to Inform Musculoskeletal Rehabilitation and Orthopedic Treatment. Doi: 10.1123/jab.2023-0029.

Kian, A., Pizzolato, C., Halaki, M., Ginn, K., Lloyd, D., Reed, D., Ackland, D., 2019. Static optimization underestimates antagonist muscle activity at the glenohumeral joint: a musculoskeletal modeling study. J. Biomech. 97, 109348. https://doi.org/10.1016/j.jbiomech.2019.109348.

Killen, B.A., Falisse, A., De Groote, F., Jonkers, I., 2020. In silico-enhanced treatment and rehabilitation planning for patients with musculoskeletal disorders: can musculoskeletal modelling and dynamic simulations really impact current clinical practice? Appl. Sci. 10, 7255. https://doi.org/10.3390/app10207255.

Klemt, C., Prinold, J.A., Morgans, S., Smith, S.H.L., Nolte, D., Reilly, P., Bull, A.M.J., 2018. Analysis of shoulder compressive and shear forces during functional activities of daily life. Clin. Biomech. (Bristol, Avon) 54, 34–41. https://doi.org/10.1016/j.clinbiomech.2018.03.006.

Lavaill, M., Martelli, S., Cutbush, K., Gupta, A., Kerr, G.K., Pivonka, P., 2023. Latarjet’s muscular alterations increase glenohumeral joint stability: a theoretical study. J. Biomech. 155, 111639. https://doi.org/10.1016/j.jbiomech.2023.111639.

Lavaill, M., Pizzolato, C., Bolsterlee, B., Martelli, S., Pivonka, P., 2024. Benchmark and Validation of State-of-the-art Muscle Recruitment Strategies in Shoulder Modellin. Doi: 10.21203/rs.3.rs-3890029/v1.

Magermans, D.J., Chadwick, E.K.J., Veeger, H.E.J., van der Helm, F.C.T., 2005. Requirements for upper extremity motions during activities of daily living. Clin. Biomech. 20, 591–599. https://doi.org/10.1016/j.clinbiomech.2005.02.006.

Martelli, S., Calvetti, D., Somersalo, E., Viceconti, M., 2015. Stochastic modelling of muscle recruitment during activity. Interface Focus 5, 20140094. https://doi.org/10.1098/rsfs.2014.0094.

Martelli, S., Calvetti, D., Somersalo, E., Viceconti, M., Taddei, F., 2013. Computational tools for calculating alternative muscle force patterns during motion: a comparison of possible solutions. J. Biomech. 46, 2097–2100. https://doi.org/10.1016/j.jbiomech.2013.05.023.

Millard, M., Uchida, T., Seth, A., Delp, S.L., 2013. Flexing computational muscle: modeling and simulation of musculotendon dynamics. J. Biomech. Eng. 135. https://doi.org/10.1115/1.4023390.

Nikooyan, A.A., Veeger, H.E.J., Westerhoff, P., Bolsterlee, B., Graichen, F., Bergmann, G., van der Helm, F.C.T., 2012. An EMG-driven musculoskeletal model of the shoulder. Human Movement Science, Special issue on Network approaches in complex environments 31, 429–447. Doi: 10.1016/j.humov.2011.08.006.

Nikooyan, A.A., Veeger, H.E.J., Westerhoff, P., Graichen, F., Bergmann, G., van der Helm, F.C.T., 2010. Validation of the delft shoulder and elbow model using *in-vivo* glenohumeral joint contact forces. J. Biomech. 43, 3007–3014. https://doi.org/10.1016/j.jbiomech.2010.06.015.

Puchaud, P., Bailly, F., Begon, M., 2023. Direct multiple shooting and direct collocation perform similarly in biomechanical predictive simulations. Comput. Methods Appl. Mech. Eng. 414, 116162. https://doi.org/10.1016/j.cma.2023.116162.

Scholz, J.P., Schöner, G., 1999. The uncontrolled manifold concept: identifying control variables for a functional task. Exp. Brain Res. 126, 289–306. https://doi.org/10.1007/s002210050738.

van Veen, B.C., Mazza, C., Viceconti, M., 2020. The uncontrolled manifold theory could explain part of the inter-trial variability of knee contact force during level walking. IEEE Trans. Neural Syst. Rehabil. Eng. 28, 1800–1807. https://doi.org/10.1109/tnsre.2020.3003559.

Veeger, D.H.E.J., C. T. van der Helm, F., Nikooyan, A.A., 2023. Kinematic and kinetic data recorded with an instrumented shoulder prosthesis. Doi: 10.4121/86DB1D7D-13D9-4631-9C6B-1E3134A1AB38.V1.

Veeger, H.E.J., Magermans, D.J., Nagels, J., Chadwick, E.K.J., van der Helm, F.C.T., 2006. A kinematical analysis of the shoulder after arthroplasty during a hair combing task. Clinical Biomechanics, Proceedings of the 5th Meeting of the International Shoulder Group 21, S39–S44. Doi: 10.1016/j.clinbiomech.2005.09.012.

Veerkamp, K., Schallig, W., Harlaar, J., Pizzolato, C., Carty, C.P., Lloyd, D.G., van der Krogt;, M.M., 2019. The effects of electromyography-assisted modelling in estimating musculotendon forces during gait in children with cerebral palsy. J. Biomech. 92, 45–53. https://doi.org/10.1016/j.jbiomech.2019.05.026.

Viceconti, M., Curreli, C., Bottin, F., Davico, G., 2021. Effect of suboptimal neuromuscular control on the risk of massive wear in total knee replacement. Ann. Biomed. Eng. 49, 3349–3355. https://doi.org/10.1007/s10439-021-02795-y.

Wickham, J., Pizzari, T., Stansfeld, K., Burnside, A., Watson, L., 2010. Quantifying ‘normal’ shoulder muscle activity during abduction. J. Electromyogr. Kinesiol. 20, 212–222. https://doi.org/10.1016/j.jelekin.2009.06.004.